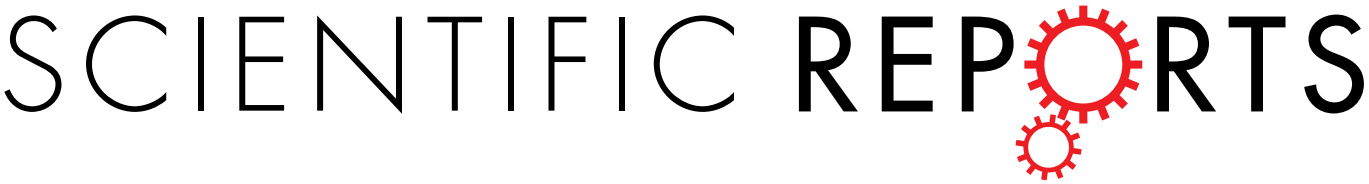

OPEN

Optical polarization and intervalley scattering in single layers of MoS_2 and $MoSe_2$

Received: 06 September 2015
Accepted: 11 April 2016
Published: 26 April 2016

G. Kioseoglou[1,2], A. T. Hanbicki[3], M. Currie[4], A. L. Friedman[3] & B. T. Jonker[3]

Single layers of MoS_2 and $MoSe_2$ were optically pumped with circularly polarized light and an appreciable polarization was initialized as the pump energy was varied. The circular polarization of the emitted photoluminescence was monitored as a function of the difference between the excitation energy and the A-exciton emission at the K-point of the Brillouin zone. Our results show a threshold of twice the LA phonon energy, specific to the material, above which phonon-assisted intervalley scattering causes depolarization. In both materials this leads to almost complete depolarization within ~100 meV above the threshold energy. We identify the extra kinetic energy of the exciton (independent of whether it is neutral or charged) as the key parameter for presenting a unifying picture of the depolarization process.

Materials often exhibit fundamentally new phenomena in reduced dimensions, and the new properties that emerge can lead to novel applications. Like graphite, the molybdenum-based transition metal dichalcogenides, MoX_2 (X = S, Se) are a class of materials that readily lend themselves to dimensional manipulation. These layered structures have strong intralayer bonding and weak interlayer van der Waals coupling, enabling one to isolate individual layers. In bulk form, MoX_2 are indirect gap semiconductors. However, because of their reduced dimensionality, single layers are direct-gap with a range of bandgaps in the visible regime. This makes them ideal candidates for a host of optoelectronic applications ranging from light-emitting diodes to light harvesting to sensors[1–5]. Besides the obvious light-based applications, these materials are also good candidates for the emerging field of valleytronics[6–12]. The reduced-dimensional, hexagonal lattice leads to non-degenerate K-points in the Brillouin zone making the inequivalent K and K' valley populations potential new state-variables of these systems.

A single layer of MoX_2, schematically shown in Fig. 1(a), consists of a plane of transition metal atoms sandwiched by layers of chalcogen atoms. The Brillouin zone of this system is shown in Fig. 1(b). In single layer form, the direct gap occurs at the K-point, and the optical properties of these materials are governed by strong excitonic transitions, both neutral and charged. These excitons are strongly bound, with the neutral exciton having binding energies on the order of 0.5–0.8 eV[13–17] and the charged exciton (trion) having a binding energy of 20–30 meV[9,18]. In addition to being optically active with strong photoluminescence (PL), they also have unique optical selection rules (Fig. 1(c)). Time reversal symmetry and strong orbital-hybridization couples the valley and spin indices. This enables access to a single valley using polarized light, since the angular momentum of incident circularly-polarized light interacts with carriers to produce specific spin states[8–11,19,20]. In other words, the symmetry properties of the two inequivalent valleys lead to a difference in the absorption of circularly polarized light, either positive (σ^+) or negative (σ^-) helicity, resulting in a strong chiral selectivity.

Polarization-resolved photoluminescence of single layer MoS_2 has been extensively studied, and a high initial circular polarization was reported with a circularly polarized pump[8,19]. In contrast, there are few polarization-dependent studies for $MoSe_2$ at zero magnetic field. One recent study[21] reported very low initial circular polarization in the PL. This result is surprising since one expects members of the MoX_2 family to behave similarly. Several other recent studies[22,23], demonstrated generation of valley polarization in $MoSe_2$ by applying external magnetic fields up to 10 T perpendicular to the sample. In particular, MacNeil *et al.*[22] observed a maximum polarization of 14% for the charged and 9% for the neutral exciton at 4.2 K and 6.7 T attributed to the magnetic field breaking the K/K' valley-degeneracy.

[1]Department of Materials Science and Technology, University of Crete, Heraklion Crete, 71003, Greece. [2]Institute of Electronic Structure and Laser (IESL), Foundation for Research and Technology Hellas (FORTH), Heraklion Crete, 71110, Greece. [3]Materials Science & Technology Division, Naval Research Laboratory, Washington, DC 20375, USA. [4]Optical Sciences Division, Naval Research Laboratory, Washington, DC 20375, USA. Correspondence and requests for materials should be addressed to G.K. (email: gnk@materials.uoc.gr) or A.T.H. (email: hanbicki@nrl.navy.mil)

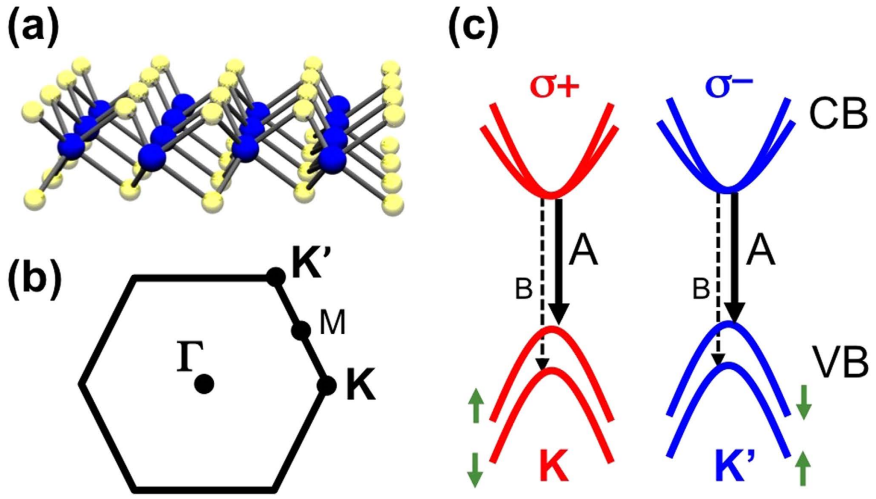

Figure 1. Structure of Monolayer MoS_2. (**a**) Crystal structure of a single-layer transition-metal dichalcogenide. A central layer of transition metal atoms is sandwiched by layers of chalcogens. (**b**) Brillouin zone for a reduced dimensional hexagonal lattice. Some relevant high symmetry points are indicated. (**c**) Schematic of the single-particle band structure at K and K' valleys. The arrows denote the A (solid line) and B (dashed line) excitons. Each valley can only be excited with a specific helicity, σ^+ or σ^-.

In this work, we measure the energy-dependent valley polarization in both MoS_2 and $MoSe_2$ under zero magnetic field, and model the polarization relaxation. We probe the valley population dynamics in $MoSe_2$ and MoS_2 by selectively populating the K and K' valleys with circularly polarized light while systematically varying the laser excitation energy. For both systems, the difference in the excitation energy and PL emission energy, $\Delta E = E_{pump} - E_{PL}$, governs the depopulation of carriers in each valley. Adding more energy above a distinct threshold characteristic of the longitudinal acoustic (LA) phonon for each material enables inter-valley scattering and produces a sharp decrease in the observed circular polarization. LA phonons in these two systems have different energies (30 meV for MoS_2 and 19 meV for $MoSe_2$)[24,25], and we show that the threshold for the excess energy required to initiate the depolarization process clearly reflects the material specific phonon energy. In addition, our results show that independent of how many carriers are excited, *i.e.* whether you create neutral or charged excitons, the scattering process is the same. We find that the key parameter for the depolarization process is the extra kinetic energy of the exciton – depolarization is due to intervalley scattering that begins to occur when the exciton energy exceeds a threshold corresponding to twice the LA phonon energy.

Results

Flakes of MoS_2 and $MoSe_2$ mechanically exfoliated from bulk crystals were used in this study. Monolayer MoX_2 regions were identified with an optical microscope (Fig. 2(a,b)) and confirmed with Raman spectroscopy at room temperature (Fig. 2(c,d)). Raman spectroscopy confirms single-layer regions through the shapes and relative positions of the out-of-plane A_{1g} and in-plane E^1_{2g} Raman active modes[26–28] (see Methods section). In Fig. 2(c) the 18 cm^{-1} splitting between E^1_{2g} (384 cm^{-1}) and A_{1g} (402 cm^{-1}) modes verifies the monolayer nature of the MoS_2 sample[26]. Raman spectra from $MoSe_2$ taken under the same conditions are shown in Fig. 2(d) for several layer thicknesses. The identification of the single layer[27] is based on the absence of the B_{2g} mode at 353 cm^{-1}, which can be clearly seen in Fig. 2(d). A micro-PL setup was used to collect the PL in a backscattering geometry (see methods section). The PL spectra were analyzed as σ^+ and σ^- using a combination of quarter-wave plate (liquid crystal retarder) and linear polarizer placed before the spectrometer entrance slit. The degree of circular polarization is defined as $P_{circ} = (I_+ - I_-)/(I_+ + I_-)$, where $I_+(I_-)$ is the intensity of the $\sigma^+(\sigma^-)$ component of the PL.

Temperature dependent PL emission from MoS_2 and $MoSe_2$ are shown in Fig. 3(a,b), respectively (full experimental details are described elsewhere)[11]. In these spectra, the samples were excited with a laser at 2.33 eV (532 nm). The dominant emission peak is the A-exciton, a feature that originates from the lowest energy transition at the K-point of the Brillouin zone (see Fig. 1(c)). At low temperature, we measure the A-exciton at 1.89 eV for MoS_2, and at 1.625 eV for $MoSe_2$ reflective of the smaller bandgap of $MoSe_2$. The width of the emission from MoS_2 is very broad (FWHM = 0.09 eV) so it is not possible to distinguish features within the spectra and we assign this feature to the neutral exciton, X^0. However, the emission from $MoSe_2$ is much narrower (FWHM = 0.01 eV), and it is possible to distinguish two clear peaks separated by 0.03 eV that become apparent as the sample is heated (Fig. 3(b)). These peaks have been identified as a neutral exciton (X^0) and a charged exciton (T)[18]. It is not possible to determine whether the lower energy peak is a positive or negative charged exciton based solely on the emission energy, because the effective mass of electrons and holes in this material is similar.

As the temperature is increased the relative luminescence of charged *vs.* neutral exciton changes, with the neutral exciton eventually becoming the dominant feature. Note that the charged exciton is still visible at temperatures much higher than is seen in other quasi-2D systems such as GaAs QWs[29]. The temperature dependence of the exciton emission channels for both systems shows a typical semiconductor behavior (Fig. 3(c,d), solid

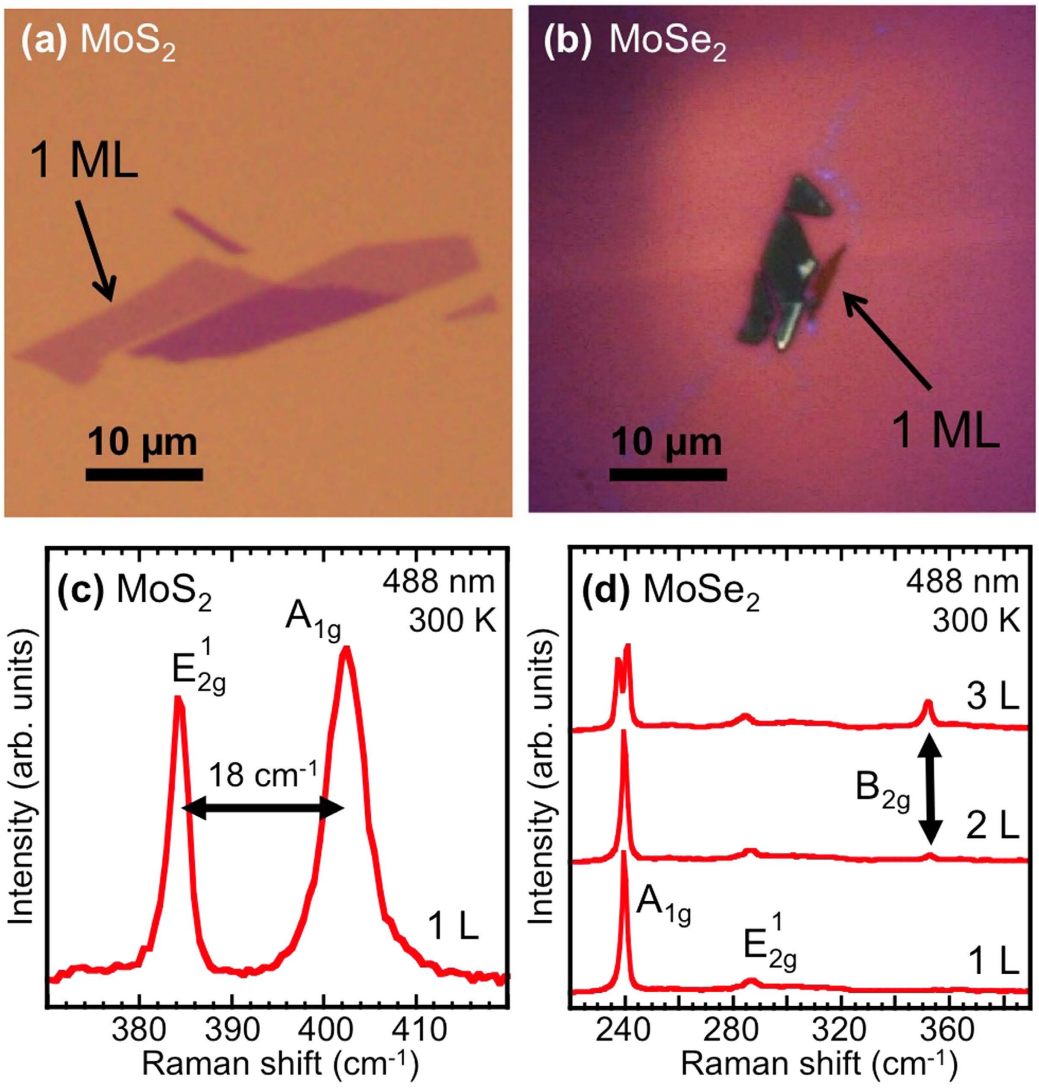

Figure 2. Characterization of single layers. Optical image of (**a**) MoS_2 and (**b**) $MoSe_2$ samples. (**c**) Raman spectrum of single layer MoS_2. The 18 cm^{-1} energy separation between the in-plane and out-of-plane modes is characteristic of single layer MoS_2. (**d**) Raman spectrum of 1, 2, and 3 layers of $MoSe_2$. Spectra are offset for clarity. The absence of the B_{2g} mode is the fingerprint for the single layer. All spectra were taken at 300 K with an excitation wavelength of 488 nm.

symbols) and the data can be fit using a standard hyperbolic cotangent relation as defined by O'Donnell and Chen[30]. The solid lines are the fits to the data with the function $E(T) = E(0) - S\langle\hbar\omega\rangle[\coth(\langle\hbar\omega\rangle/2kT) - 1]$ where $E(0)$ is the energy position of a given feature at zero temperature, S is a dimensionless coupling constant, and $\langle\hbar\omega\rangle$ is an average phonon energy. The fitting parameters obtained here are $S = 1.16$ (2.18) and $\langle\hbar\omega\rangle = 19$ meV (14.5 meV) for MoS_2 ($MoSe_2$).

To examine the valley spin dynamics, we measure the helicity dependent PL from these monolayers. Because of the optical selection rules (Fig. 1(c)), when pumped with light of positive (σ^+) or negative (σ^-) helicity, either the K or K' valley will be selectively populated[6]. Information on the depolarization process comes from analyzing the polarization of the subsequent PL. Figure 4(a,b) show representative PL spectra analyzed for σ^+ (solid red line) and σ^- (dashed blue line) at T = 5 K for MoS_2 and $MoSe_2$, respectively, at selected σ^+ excitation energies. By using a combination of sharp, long-pass filters, stray light was suppressed at the spectrometer entrance. In addition, as the excitation energy approached the PL emission energy, the excited Raman modes were cut-off from entering the detection system. This experimental setup limited our lowest excitation energies to 1.984 eV (625 nm) for MoS_2 and 1.722 eV (720 nm) for $MoSe_2$. It is clear from Fig. 4 that, for both materials, the higher the excitation energy, the lower the polarization of the emission[31].

The degree of circular polarization is shown in Fig. 5 as a function of the excess energy, $\Delta E = E_{pump} - E_{PL}$, the difference between the excitation energy E_{exc} and PL emission energy, E_{PL} (the inset of Fig. 5 is a graphical representation). Data are plotted for $MoSe_2$ (solid red circles) and MoS_2 (solid blue circles) and are derived from spectra where the temperature was held constant and the laser energy was varied, or the laser energy was fixed

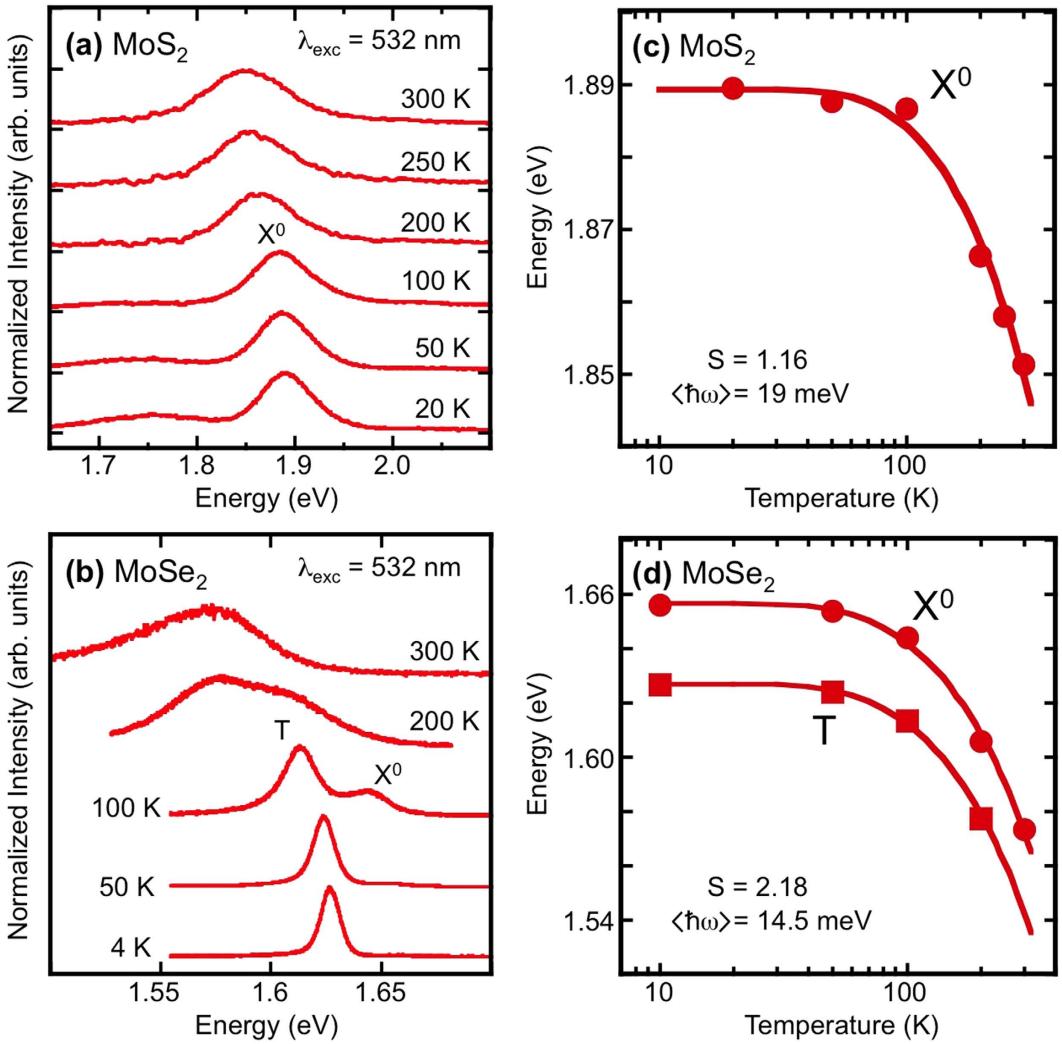

Figure 3. Temperature dependence of photoluminescence. Normalized PL spectra for (**a**) MoS_2 and (**b**) $MoSe_2$ taken with unpolarized 532 nm excitation at selected temperatures. Spectra are offset for clarity. Temperature dependent shift of the exciton emission energy in (**c**) MoS_2 and (**d**) $MoSe_2$.

and the emission energy was varied via a change in temperature[8,11,19]. Since this plot incorporates the energy difference between excitation and PL emission rather than the specific energy of the neutral and charged excitons, the behavior observed for both materials can be shown. Data for MoS_2 from the literature are also plotted in Fig. 5. The open circle, open square with a cross, and open triangle are data from Refs 8,10 and 20, respectively. These data were taken at 5 K with circularly polarized excitation from a HeNe laser (1.96 eV). The open squares with a slash are data from Ref 19 obtained at fixed excitation energy of 1.96 eV but at temperatures ranging from 5 to 300 K. To the best of our knowledge, these data represent the trends seen in the literature for MoS_2. All data follow the same depolarization trend line when plotted as a function of excess energy. Using this methodology, all of the data collapse onto a single curve for each material, independent of whether the polarization of the trion or neutral exciton is considered. The data clearly demonstrate that as the excess energy increases the emitted circular polarization decreases.

Discussion

To explain this behavior, we begin by noting that due to the optical selection rules[6] intra-valley scattering cannot result in a reduction in the observed polarization even if the pump energy exceeds the spin-orbit splitting (160 meV for MoS_2, 180 meV for $MoSe_2$)[8]. Therefore, inter-valley scattering is required to account for the reduced polarization observed, and the change in momentum necessary for such scattering implicates a phonon-mediated process[8,11]. Close to resonance the emitted circular polarization is expected to be essentially 100%, since there is not enough energy in the system to facilitate intervalley scattering. As the laser excitation energy increases or as the temperature changes for a fixed pumping energy, the available excess energy ΔE increases and phonon-assisted scattering is enabled above some material-dependent energy threshold. For MoS_2, the combined data set clearly interpolate to 100% polarization at $\Delta E = 60$ meV, corresponding to twice the LA phonon energy[11].

Intervalley scattering requires participation from in-plane longitudinal phonons. From the phonon-dispersion curves for single layers of MoS_2 and $MoSe_2$ the lowest energy phonon available for scattering are longitudinal

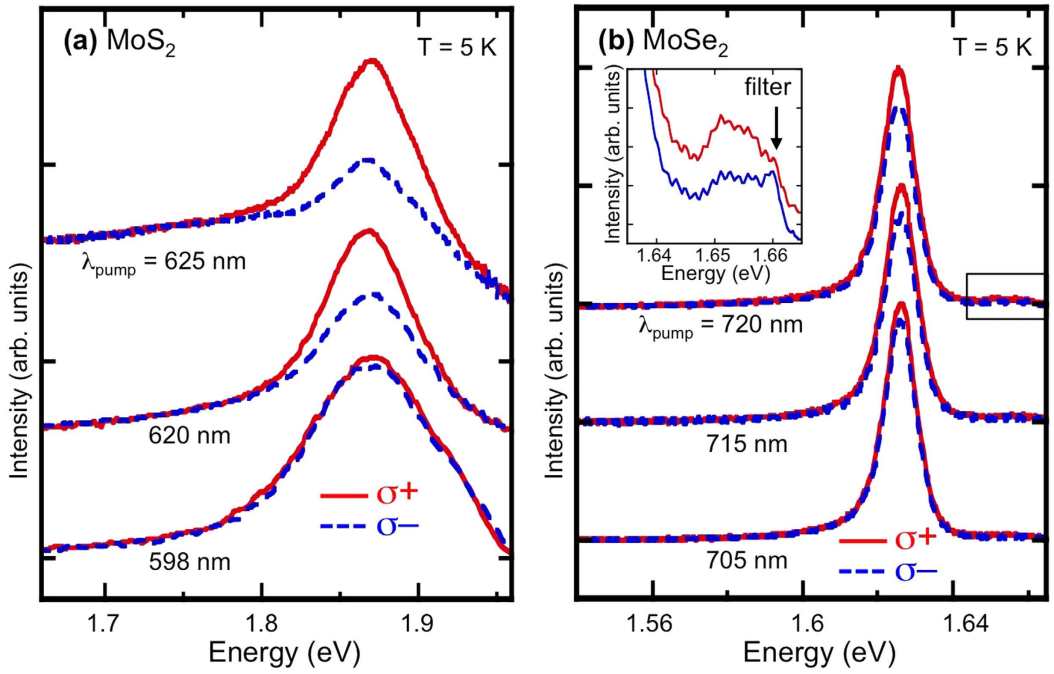

Figure 4. Polarization of photoluminescence spectra. PL spectra at T = 5 K analyzed for σ^+ and σ^- at selected photo-excitation energies for (**a**) MoS_2 and (**b**) $MoSe_2$. The pumping is σ^+ in both cases. A dramatic decrease in the emitted circular polarization is observed as the excitation energy increases. The peaks were normalized and vertically shifted for clarity. For the $MoSe_2$ spectra, the inset is an enlargement of the area indicated by a rectangular box and shows the neutral exciton emission.

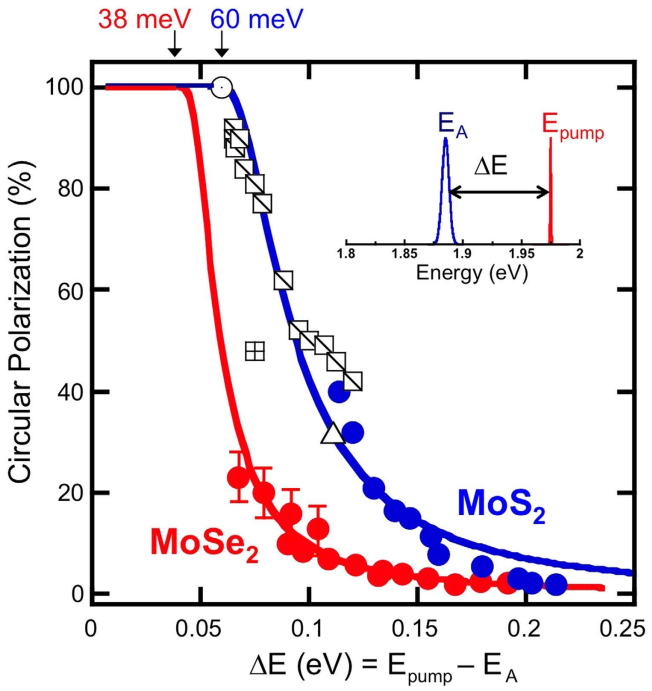

Figure 5. Polarization dependence on excess energy. Degree of circular polarization of the emitted PL as function of excess energy, ΔE. Data are derived from spectra where the temperature was held constant and the laser energy was varied, or the laser energy was fixed and the emission energy was varied via a change in temperature. Solid symbols ($MoSe_2$ is red and MoS_2 is blue) are our data, and open symbols are data from references 8,10,19,20. A graphical definition of excess energy is presented in the inset. Except where noted, error bars are not in excess of the symbol size.

acoustic phonons with energies of 30 meV for MoS_2[24] and 19 meV for $MoSe_2$[25]. Intervalley scattering becomes accessible when the excitation energy exceeds a threshold value that is the sum of the exciton Coulombic formation energy (PL emission energy) and twice the lowest acoustic-phonon energy available in the system (essentially a phonon for each the electron and hole). That is 60 meV for MoS_2 and 38 meV for $MoSe_2$. There are two mechanisms that could be responsible for the electron or hole spin-flip during this phonon mediated intervalley scattering event. One is that the spin-flip is mediated by short range scattering from impurities. The presence of a background carrier population could enhance the probability of such a process[31]. The other mechanism is that intervalley scattering proceeds through the nearly spin-degenerate Γ valley of the Brillioun zone[32].

The $MoSe_2$ data (solid red symbols) exhibit a similar behavior – the measured polarization rapidly increases as the excess energy ΔE decreases. The narrow linewidths in $MoSe_2$ allow us to distinguish the particular emission channels X^0 and T. Therefore, for $MoSe_2$, we can plot the polarization of both the neutral and charged exciton. Note that due to the low intensity of the X^0 data, it is difficult to see the polarization on the same scale as the trion emission, therefore a typical set of X^0 emission spectra are shown in the inset of Fig. 4(b). As with MoS_2, all the data coalesce onto the same depolarization curve as a function of excess energy. The solid red line is a model fit described below, and intercepts 100% polarization at $\Delta E = 38$ meV, corresponding to twice the $MoSe_2$ LA phonon energy of 19 meV from the literature[25]. These data make it clear that depolarization and intervalley scattering are governed by the excess energy, ΔE, imparted to the photoexcited carriers through optical pumping.

To model this behavior, we begin with a familiar rate equation model in which the emitted circular polarization can be expressed as $P_{circ} = 1/\left(1 + 2\frac{\tau_r}{\tau_s}\right)$, where τ_r is the exciton lifetime and τ_s the intervalley scattering time[8,11]. Both τ_r and τ_s depend on temperature, or more specifically on the thermal energy given to the exciton during optical excitation. We associate this additional thermal energy with the excess energy, ΔE. It has been shown that τ_r depends linearly on temperature[33], therefore we expect it to have a linear dependence with ΔE. In addition, the increase in the excess energy leads to an increase of the phonon population. We assign the intervalley scattering rate τ_s^{-1} to be proportional to the phonon population $\langle n \rangle = 1/(e^{\hbar\omega_q/kT} - 1)$ and substitute kT with $(\Delta E - \hbar\omega_q)$. Taking into account these dependencies on ΔE we can fit the data using the relation $P = 1/(1 + C\Delta E/(e^{\hbar\omega_q/(\Delta E - \hbar\omega_q)} - 1))$. Here $\hbar\omega_q$ is twice the LA phonon energy, the minimum energy necessary for the exciton (electron and hole) to scatter from one valley to the other and reduce the optical polarization, and C is a scaling constant. These two values, C and $\hbar\omega_q$, are the only fitting parameters. Note that this fitting relation is valid only for $\Delta E > \hbar\omega_q$. The solid lines in Fig. 5 are fits to the data and yield values for 2LA of 54 meV for MoS_2 and 38 ± 4 meV for the $MoSe_2$, in good agreement with the respective literature values of 60 and 38 meV[24,25]. The data for MoS_2 diverge systematically from the fitted line above 150 meV. The main reason for this discrepancy may be that our simple rate equation model does not take into account the spin-orbit interaction (150 meV for MoS_2)[11].

Even though the optical response of 2-dimensional crystals is dominated by the formation of excitons, we used the phonon-assisted intervalley scattering model, which is based on a single particle picture. This is a straightforward way to describe the sharp depolarization of the emitted PL as a function of the excess energy that includes a threshold energy. However, the thermally activated relaxation of the carriers may not represent all aspects of physics that could describe the spin relaxation in this system. Recently, alternative interpretations based on the excitonic picture explain the PL depolarization as valley-decoherence due to long-range exciton exchange, *i.e.* direct intervalley electron-hole exchange[32,34–38]. Both of these mechanisms may be at play with different relative contributions that varies across different material systems. Our observation of a threshold depolarization energy, however, is more easily explained with the phonon model we have presented.

In summary, at zero magnetic field, we initialized circular polarization in MoS_2 and $MoSe_2$ using energy-dependent circularly-polarized optical pumping and measured the valley polarization process as a function of the excess energy absorbed by the carriers. Independent of the emission channel or the material studied (MoS_2 or $MoSe_2$), all the data can be modeled by a single depolarization mechanism, intervalley scattering mediated by LA phonons. The threshold needed for depolarization is found to be twice the LA phonon energy of the corresponding material, and the exciton kinetic energy greater than this is the key parameter for the depolarization. Generating high chirality photoluminescence in Mo-based two-dimensional structures enables applications in valley-photonics.

Methods

Sample preparation and characterization. All samples used in this study were mechanically exfoliated from bulk crystals. The MoS_2 was deposited onto a 285-nm SiO_2 layer on a Si substrate, while the $MoSe_2$ flakes were deposited on a 90-nm SiO_2 layer on a Si substrate. The typical size of monolayer regions are 5–10 μm across for MoS_2 and 1–2 μm for $MoSe_2$ and were identified with an optical microscope and confirmed with Raman spectroscopy at room temperature and 488 nm excitation. Raman spectroscopy has been established as a reliable tool for determining the specific number of layers in transition metal dichalcogenides[26–28]. In MoS_2, the 18 cm^{-1} energy difference between the two main vibrational modes, E^1_{2g} at 384 cm^{-1} and A_{1g} at 402 cm^{-1}, is the fingerprint for the accurate determination of the single layer. In $MoSe_2$, the in-plane E^1_{2g} (287 cm^{-1}) and the out-of-plane A_{1g} (242 cm^{-1}) modes are much lower in energy than in MoS_2 because of the larger mass of the Se atom. Also, the in-plane and out-of-plane modes switch positions relative to the MoS_2, i.e, the out-of-plane mode is softer than the in-plane one. This can be verified by measuring thicker layers of $MoSe_2$ and observing a Davydov splitting in the A_{1g} mode for multi-layer flakes. The single layer is identified by the absence of the B_{2g} mode at 353 cm^{-1}.

Optical measurements. The photoluminescence data were taken in a backscattering geometry using a micro-PL setup (spatial resolution of 1 μm) with a 50× objective and incorporating a continuous-flow He-cryostat. The MoS_2 samples were excited with either a continuous-wave 2.33 eV (532 nm) solid-state laser or

a tunable pulsed laser while the $MoSe_2$ flakes were excited by a continuous-wave Ti:Sapphire laser. The pulsed source was an optical parametric amplifier (pumped by a Ti:Sapphire laser) tunable from 1.77–2.48 eV (700–500 nm) at a 250-kHz repetition rate with a double-pass grating (500 g/mm) geometry to reduce the spectral bandwidth to <5 meV (1 nm). The photoluminescence emission was collected, passed though a polarization analyzer, and dispersed by a single monochromator equipped with a multichannel charge coupled device (CCD) detector.

References

1. Mak, K. F., Lee, C., Hone, J., Shan, J. & Heinz, T. F. Atomically Thin MoS_2: A New Direct-Gap Semiconductor. *Phys. Rev. Lett.* **105,** 136805 (2010).
2. Splendiani, A. *et al.* Emerging Photoluminescence in Monolayer MoS_2. *Nano Lett.* **10,** 1271–1275 (2010).
3. Korn, T., Heydrich, S., Hirmer, M., Schmutzler, J. & Schüller, C. Low-temperature photocarrier dynamics in monolayer MoS_2. *Appl. Phys. Lett.* **99,** 102109 (2011).
4. Bernardi, M., Palummo, M. & Grossman, J. C. Extraordinary Sunlight Absorption and One Nanometer Thick Photovoltaics Using Two-Dimensional Monolayer Materials. *Nano Letters* **13,** 3664–3670 (2013).
5. Perkins, F. K. *et al.* Chemical Vapor Sensing with Monolayer MoS_2. *Nano Letters* **13,** 668–673 (2013).
6. Xiao, D., Liu, G.-B., Feng, W., Xu, X. & Yao, W. Coupled Spin and Valley Physics in Monolayers of MoS_2 and Other Group-VI Dichalcogenides. *Phys. Rev. Lett.* **108,** 196802 (2012).
7. Zhu, Z. Y., Cheng, Y. C. & Schwingenschlögl, U. Giant spin-orbit-induced spin splitting in two-dimensional transition-metal dichalcogenide semiconductor. *Phys. Rev. B* **84,** 153402 (2011).
8. Mak, K. F., He, K., Shan, J. & Heinz, T. F. Control of valley polarization in monolayer MoS_2 by optical helicity. *Nat. Nanotechnol.* **7,** 494–498 (2012).
9. Mak, K. F. *et al.* Tightly bound trions in monolayer MoS_2. *Nat. Mater.* **12,** 207–211 (2012).
10. Cao, T. *et al.* Valley-selective circular dichroism of monolayer molybdenum disulphide. *Nat. Commun.* **3,** 887 (2012).
11. Kioseoglou, G. *et al.* Valley polarization and intervalley scattering in monolayer MoS_2. *Appl. Phys. Lett.* **101,** 221907 (2012).
12. Davelou, D., Kopidakis, G., Kioseoglou, G. & Remediakis, I. N. MoS_2 nanostructures: Semiconductors with metallic edges. *Solid State Comm.* **192,** 42–46 (2014).
13. Qiu, D. Y., da Jornada, F. H. & Louie, S. G. Optical Spectrum of MoS2: Many-Body Effects and Diversity of Exciton States. *Phys. Rev. Lett.* **111,** 216805 (2013).
14. Hanbicki, A. T., Currie, M., Kioseoglou, G., Friedman, A. L. & Jonker, B. T. Measurement of high exciton binding energy in the monolayer transition-metal dichalcogenides WS_2 and WSe_2. *Solid State Commun.* **203,** 16–20 (2015).
15. Ramasubramaniam, A. Large excitonic effects in monolayers of molybdenum and tungsten dichalcogenides. *Phys. Rev. B* **86,** 115409 (2012).
16. He, K. *et al.* Tightly Bound Excitons in Monolayer WSe_2. *Phys. Rev. Lett.* **113,** 026803 (2014).
17. Chernikov, A. *et al.* Exciton Binding Energy and Nonhydrogenic Rydberg Series in Monolayer WS_2. *Phys. Rev. Lett.* **113,** 076802 (2014).
18. Ross, J. S. *et al.* Electrical control of neutral and charged excitons in a monolayer semiconductor. *Nature Communications* **4,** 1474 (2013).
19. Sallen, G. *et al.* Robust optical emission polarization in MoS_2 monolayers through selective valley excitation. *Phys. Rev. B* **86,** 081301R (2012).
20. Zeng, H., Dai, J., Yao, W., Xiao, D. & Cui, X. Valley polarization in MoS_2 monolayers by optical pumping. *Nat. Nanotechnol.* **7,** 490–493 (2012).
21. Wang, G. *et al.* Polarization and time-resolved photoluminescence spectroscopy of excitons in $MoSe_2$ monolayers. *Appl. Phys. Lett.* **106,** 112101 (2015).
22. MacNeil, D. *et al.* Breaking of Valley Degeneracy by Magnetic Field in Monolayer $MoSe_2$. *Phys. Rev. Lett.* **114,** 037401 (2015).
23. Li, Y. *et al.* Valley Splitting and Polarization by the Zeeman Effect in Monolayer $MoSe_2$. *Phys. Rev. Lett.* **113,** 266804 (2014).
24. Molina-Sánchez, A. & Wirtz, L. Phonons in single-layer and few-layer MoS_2 and WS_2. *Physical Review B* **84,** 155413 (2011).
25. Horzum, S. *et al.* Phonon Softening and direct to indirect band gap crossover in strained single-layer $MoSe_2$. *Phys. Rev. B* **87,** 125415 (2013).
26. Lee, C. *et al.* Anomalous Lattice Vibrations of Single-and Few-Layer MoS_2. *ACS Nano* **4,** 2695–2700 (2010).
27. Tonndorf, P. Photoluminescence emission and Raman response of monolayer MoS_2, $MoSe_2$, and WSe_2. *Optics Express* **21,** 4908–4916 (2013).
28. Tongay, S. *et al.* Thermally Driven Crossover from Indirect toward Direct Bandgap in 2D Semiconductors: $MoSe_2$ versus MoS_2. *Nano Lett.* **12,** 5576–5580 (2012).
29. Kioseoglou, G. *et al.* Photoluminescence and reflectance studies of negatively charged excitons in GaAs/AlGaAs quantum-well structres. *Phys. Rev. B* **61,** 4780 (2000).
30. O'Donnell, K. P. & Chen, X. Temperature dependence of semiconductor band gaps. *Appl. Phys. Lett.* **58,** 2924 (1991).
31. Song, Y. & Dery, H. Transport Theory of Monolayer Transition-Metal Dichalcogenides through Symmetry. *Phys. Rev. Lett.* **111,** 026601 (2013).
32. Mai, C. *et al.* Many-Body Effects in Valleytronics: Direct Measurement of Valley Lifetimes in Single-Layer MoS_2. *Nano Lett.* **14,** 202–206 (2014).
33. Palummo, M., Bernardi, M. & Grossman, J. C. Exciton Radiative Lifetimes in Two-Dimensional Transition Metal Dichalcogenides. *Nano Lett.* **15,** 2794–2800 (2015).
34. Glazov, M. M. *et al.* Exciton fine structure and spin decoherence in monolayers of transition metal dichalcogenides. *Phys. Rev. B* **89,** 201302 (2014).
35. Yu, T. & Wu, M. W. Valley depolarization due to intervalley and intravalley electron-hole exchange interactions in monolayer MoS_2. *Phys. Rev. B* **89,** 205303 (2014).
36. Dery, H. & Song, Y. Polarization analysis of excitons in monolayer and bilayer transition-metal dichalcogenides. *Phys. Rev. B* **92,** 125431 (2015).
37. Glazov, M. M. *et al.* Spin and valley dynamics of excitons in transition metal dichalcogenide monolayers. *Phys. Status Solidi B* **252,** 2349–2362 (2015).
38. Dal Conte, S. *et al.* Ultrafast valley relaxation dynamics in monolayer MoS_2 probed by nonequilibrium optical techniques. *Phys. Rev. B* **92,** 235425 (2015).

Acknowledgements

We would like to thank Jim Culbertson for assistance with Raman measurements. G.K. gratefully acknowledges the hospitality and support of the Naval Research Laboratory where the experiments were performed. This work was supported by core programs at NRL and the NRL Nanoscience Institute, and by Air Force Office of Scientific Research under contract number F4GGA24233G001.

Author Contributions

G.K., A.H. and M.C. performed the experiments. G.K., A.H. and M.C. analyzed the data. A.F. fabricated the samples. All authors discussed the results and A.H., G.K., M.C. and B.J. wrote the manuscript.

Additional Information

Competing financial interests: The authors declare no competing financial interests.

How to cite this article: Kioseoglou, G. *et al.* Optical polarization and intervalley scattering in single layers of MoS_2 and $MoSe_2$. *Sci. Rep.* **6**, 25041; doi: 10.1038/srep25041 (2016).